ChemComm

Accepted Manuscript

This article can be cited before page numbers have been issued, to do this please use: X. Li, M. Liu, Y. Li, X. Cai, D. Chen, K. Liu, Y. CAO and S. Su, *Chem. Commun.*, 2016, DOI: 10.1039/C6CC08501F.

This is an Accepted Manuscript, which has been through the Royal Society of Chemistry peer review process and has been accepted for publication.

Accepted Manuscripts are published online shortly after acceptance, before technical editing, formatting and proof reading. Using this free service, authors can make their results available to the community, in citable form, before we publish the edited article. We will replace this Accepted Manuscript with the edited and formatted Advance Article as soon as it is available.

You can find more information about Accepted Manuscripts in the author guidelines.

Please note that technical editing may introduce minor changes to the text and/or graphics, which may alter content. The journal's standard Terms & Conditions and the ethical guidelines, outlined in our author and reviewer resource centre, still apply. In no event shall the Royal Society of Chemistry be held responsible for any errors or omissions in this Accepted Manuscript or any consequences arising from the use of any information it contains.

View Article Online
DOI: 10.1039/C6CC08501F

Journal Name

COMMUNICATION

Structure-Simplified and Highly Efficient Deep Blue Organic Light-Emitting Diodes with Reduced Efficiency Roll-Off at Extremely High Luminance†

Received 00th January 20xx,
Accepted 00th January 20xx

DOI: 10.1039/x0xx00000x

www.rsc.org/

Xiang-Long Li††, Ming Liu††, Yunchuan Li, Xinyi Cai, Dongcheng Chen, Kunkun Liu, Yong Cao and Shi-Jian Su*

Based on a series of new fluorescent emitters, deep blue non-doped multilayer OLEDs with EQE exceeding 5.10% and single layer devices excluding any charge carrier transporting materials with an EQE of 4.22% were achieved at extremely high luminance of 10000 cd m^{-2}.

In the past decades of years, numerous efforts have been devoted to developing deep blue emitters, and impressive external quantum efficiency (EQE) has been achieved particularly in development of noble metal containing phosphorescent materials[1] and thermal activated delayed fluorescence (TADF) materials.[2] However, a significant drawback of previously demonstrated deep blue OLEDs is that they are subjected to a pronounced EQE roll-off at practical display and illumination relevant high luminance.[3] Recently, outstanding works have been reported on high performance deep blue phosphorescent and TADF emitters, but the limited maximum luminance (< 10000 cd m^{-2}) confined their applications.[4] Moreover, deep blue phosphorescent and TADF devices require appropriate hosts and other functional materials with enough high triplet energy level for exciton confinement, and device structures turn out to be complicated, which is undesirable for realization of simple device fabrication process and low cost commercial production. Among conventional fluorescent emitters, materials based on triplet-triplet annihilationm (TTA) mechanism can be potential for the capability of efficient triplet exciton fussion process, yielding theoretically maximum internal quantum efficiency (IQE) of 62.5%, and can realize high efficiency at high luminance. Nevertheless, the undesired hosts hunting and complicated device doping process are also indispensable.[5]

In this communication, a group of deep blue fluorescent emitters were designed and synthesized for non-doped electroluminescent (EL) devices. For the multilayer non-doped devices, all of the deep blue fluorophores exhibited excellent EQEs exceeding 5.10% at 10000 cd m^{-2}. As for the simplified OLEDs excluding carrier transporting layers, a peak EQE of 5.12% was achieved with Commission Internationale de L'Eclairage (CIE) coordinates of (0.146, 0.106), and the EQE can be maintained at 4.22% at 10000 cd m^{-2}. Representive works were shown in **Table S1** for a clear comparison (some data were not shown directly in the references and they were fetched from the exhibited figures reasonably), which can show the excellence of our current work.

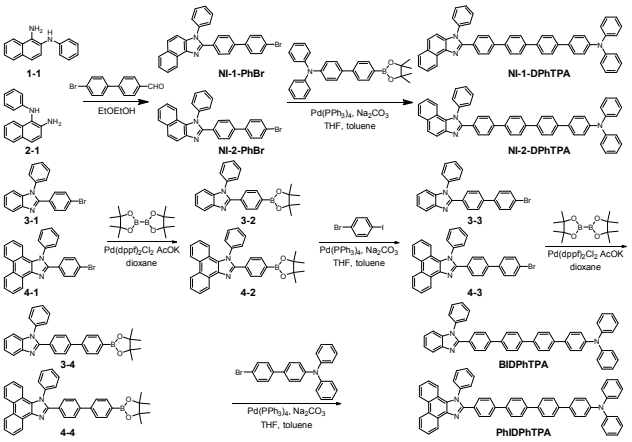

Scheme 1. Molecular structures and synthetic routes of the developed deep blue fluorescent emitters NI-1-DPhTPA, NI-2-DPhTPA, BIDPhTPA, and PhIDPhTPA.

A general electron-rich group triphenylamine (TPA) was utilized to construct all of these fluorophors, and three para interconnected benzene rings between TPA and electron-poor imidazole derivative groups play a role of link unit. Molecular structures of these newly designed and synthesized emitters, NI-1-DPhTPA, NI-2-DPhTPA, BIDPhTPA, and PhIDPhTPA, and their synthetic routes are shown in **Scheme 1**. All of these molecules were thoroughly characterized by ^{1}H, ^{13}C NMR spectrometry, and mass spectrometry. Density functional theory (DFT) calculations were performed to evaluate their

State Key Laboratory of Luminescent Materials and Devices, Institute of Polymer Optoelectronic Materials and Devices, South China University of Technology, Guangzhou, 510640, P. R. China. E-mail: mssjsu@scut.edu.cn

† Electronic Supplementary Information (ESI) available. See DOI: 10.1039/x0xx00000x

†† X.-L. Li and M. Liu contributed equally to this work.

View Article Online
DOI: 10.1039/C6CC08501F

frontier molecular orbitals and energy band gaps (**Figure S1** and **Table S2**). Although different imidazole derivatives were adopted, the calculated lowest unoccupied molecular orbitals (LUMOs) are quite similar, and also are the highest occupied molecular orbitals (HOMOs) because of the same electron-rich TPA unit. On the basis of the theoretical calculation, the synthesized compounds were also predicted to exhibit quite approximate energy band gap (E_g) and singlet excited energy (S_1) in comparison with each other (Table S2).

These compounds show quite good thermal stability for application in EL devices, as indicated by high glass transition temperatures (T_g) of 139.5, 136.6, 119.6, and 148.5 ^{o}C recorded by differential scanning calorimetry (DSC) thermograms and decomposition temperatures (T_d, corresponding to 5% weight loss) of 500.3, 448.5, 440.4, and 502.6 ^{o}C obtained from thermogravimetric analyses (TGA) for NI-1-DPhTPA, NI-2-DPhTPA, BIDPhTPA, and PhIDPhTPA, respectively (**Figure S2**).

Cyclic voltammograms (CV) were taken to estimate their HOMO levels. Each of them displayed reversible oxidated wave, which could be attributed to the oxidation of the TPA unit (**Figure S3**). HOMO levels of these compounds were calculated from the onset oxidation potential (E_{ox} vs. ferrocene/ferrocenium) and determined to be almost the same (-5.17 ~ -5.18 eV), due to the same electron rich unit.

Their representative UV-vis absorption and PL spectra were studied in various solvents, as shown in **Figure S4**, and some key data are summarized in **Table S3**. Firstly, insignificant changes were found in their absorption spectra with the increase of solvent polarity, indicating negligible polarity change at the ground state in different solvents. Secondly, all the compounds show deep blue emission at 418-420 nm with obvious vibronic structure features in low-polarity toluene solutions, while in higher polarity solutions, their PL spectra were broadened and gradually bathochromic-shifted without vibronic structure features. When the solvent polarity was increased gradually from low-polarity toluene to high-polarity dichloromethane (DCM), the compounds exhibited large red-shift of 43-47 nm. The large solvatochromic shift, which is commonly consistent with the large dipole moment of the charge transfer (CT) state, indicates that the low-lying excited state, S1, of the compounds possesses a CT-state characteristic, and tiny stronger CT-state hallmarks of the current four molecules when compared with their anolagues with less conjugated benzene rings,[6] which means the emission color of these molecules should be preserved. Comparing the absorption spectra in solid films (**Figure S5**) with those in toluene solutions, an obviously broader intramolecular charge transfer (ICT) band and slight red-shift of the absorption peak can be discovered for all of these compounds. These phenomena imply that the emitters reported herein in solid film states form compact stacking structure. The optical energy band gaps (E_g^{opt}) of NI-1-DPhTPA, NI-2-DPhTPA**,** BIDPhTPA, and PhIDPhTPA were determined to be 2.83, 2.83, 2.89, and 2.89 eV, respectively, according to the onset of absorptions in solid films. Their photophysical data are shown in **Table S3**. Their LUMO levels were estimated from their HOMO levels and E_g^{opt}s to be -2.35, -2.35, -2.28, and -2.28 eV, respectively. Finally, all the molecules reported herein show high photoluminescence quantum yields (PLQYs) of almost 100% in DCM solutions at a uniform concentration of 1×10^{-5} M, while for NI-1-DPhTPA, the PLQY in solid film declines sharply to 53%, showing severe quenching effect. DFT optimized molecular configurations indicate easier molecular stacking may occur in NI-1-DPhTPA solid film (**Figure S6**), which would result in quenching and thus a much lower PLQY. In contrast, high PLQYs of 81-85% were observed for the other molecules in solid films.

In order to probe their EL properties, non-doped multilayer OLEDs were initially investigated in a configuration of indium tin oxide (ITO)/ NPB (40 nm)/ TCTA (5 nm)/ emitter (20 nm)/ TPBi (40 nm)/ LiF (1 nm)/ Al. In these devices, N,N'-bis(naphthalen-1-yl)-N,N'-bis(phenyl)-benzidine (NPB) and 4,4',4''-tris(carbazol-9-yl)triphenylamine (TCTA) serve as a hole-transporting and an electron-blocking layer, respectively, and 2,2',2''-(1,3,5-benzinetriyl)-tris(1-phenyl-1-H-benzimidazole) (TPBi) serves as an electron-transporting and hole-blocking layer, and the emitter is NI-2-DPhTPA (marked as M1), BIDPhTPA (marked as M2) or PhIDPhTPA (marked as M3), NI-1-DPhTPA is precluded here due to its relatively poor PLQY (its EL performance can be seen in **Figure S7** and **Table S4**). Current density-voltage-luminance (J-V-L), EQE and power efficiency (PE) versus luminance characteristics and other key parameters of the multilayer devices are shown in **Figure 1** and **Table 1**.

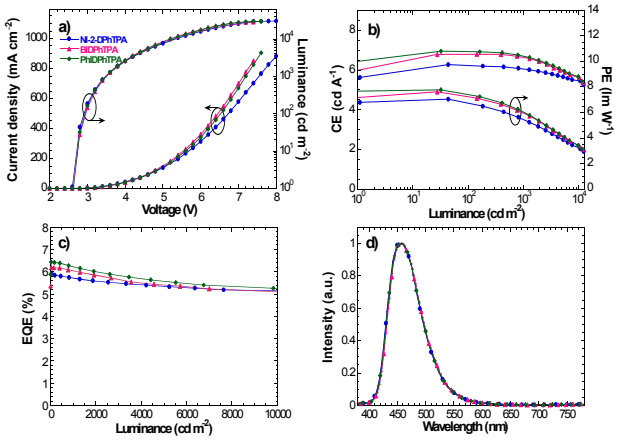

Figure 1. a) Current density and luminance versus driving voltage (J-V-L), b) current efficiency and power efficiency versus luminance (CE-L-PE), c) external quantum efficiency versus luminance (EQE-L) characteristics, and d) electroluminescence (EL) spectra at 10 mA cm^{-2} for the non-doped multilayer OLEDs in a structure of ITO/ NPB (40 nm)/ TCTA (5 nm)/ emitter (20 nm)/ TPBi (40 nm)/ LiF (1 nm)/ Al, where emitter is NI-2-DPhTPA (●, marked as M1), BIDPhTPA (▲, marked as M2), or PhIDPhTPA (◆, marked as M3).

The EQEs are 5.15, 5.10, and 5.26% at an extremely high luminance of 10000 cd m^{-2} (corresponding to current efficiencies (CE) of 5.46, 5.61, and 5.67 cd A^{-1}) for the NI-2-DPhTPA, BIDPhTPA, and PhIDPhTPA based devices, respectively. Such high values at high luminance for non-doped deep blue OLEDs have never been reported before to our best

View Article Online
DOI: 10.1039/C6CC08501F

knowledge. Especially, another excellent character of the fabricated devices is their maximum power efficiency (PE) of 7.04, 7.62, and 7.79 lm W^{-1}, which still can be kept at 5.44, 5.96, and 6.01 lm W^{-1} at 1000 cd m^{-2}, and 3.21, 3.39, and 3.43 lm W^{-1} at 10000 cd m^{-2} for the emitters NI-2-DPhTPA, BIDPhTPA, and PhIDPhTPA, respectively. The high PE values for deep blue OLEDs benifit from the extremely low driving voltages of these devices (Figure 1, Table 1). As can been seen in Table 1, a turn-on voltage as low as 2.6 V and driving voltages as low as 5.3 ± 0.1 V at 10000 cd m^{-2} have been observed.

Besides the impressive efficiencies at high luminance, the peak EQEs of the non-doped multilayer OLEDs can also reach up to 5.92, 6.18, and 6.43% for the NI-2-DPhTPA, BIDPhTPA, and PhIDPhTPA based devices, respectively. The wonderful peak values can compare favourably with the best result of the non-doped blue fluorescent devices published recently.[6a, 7] Along with the excellent maximum values, the high efficiencies at 10000 cd m^{-2} indicate that all the multilayer devices exhibit extremely low efficiency roll-off uniformly, and this could be attributed to excellent carrier balance in virtue of the felicitous molecular design. Single-carrier devices with multilayer structure were fabricated to understand the tiny efficiency roll-off of the multilayer devices. As can be seen from their current density-voltage (J-V) characteristics in **Figure 2a**, the hole current and the electron current of each emitter is pretty similar, which reveals that holes and electrons injected into the emission layers are very balanced. To gain further insights into the observed high peak efficiency, lifetimes of the compounds in DCM solutions with a uniform concentration of 1×10^{-5} M were measured firstly. All the solutions present very short lifetimes (1.32 ~ 1.79 ns, **Figure S8a**), making it clear that these emitters are totally different from the TADF materials in the inherent device operating mechanism. Short lifetimes (1.67 ~ 3.10 ns, **Figure S8b**) of neat solid films can prove the conclusion further. Additionally, the EL characters of these devices indicate that the high efficiencies cannot be attributed to TTA effect either. Firstly, the EQE versus luminance (EQE-L) curves show a slight decrease in efficiency for higher luminance (**Figure 1c**). Another evidence to oppose TTA effect, which is a second-order process proportional to the square of the triplet exciton concentration, is that the dependence of luminance on current density as shown in **Figure S9** is almost a linear curve at low injection current density. In addition, the luminance increased slower than the current density, which cannot surport TTA again.[8] Considering the excellent comprehensive device performance, a miraculous balance of low driving voltages, highly efficiency, deep blue emission, and extremely low efficiency roll-off was realized simultaneously, making the current non-doped blue OLEDs very shining herein.

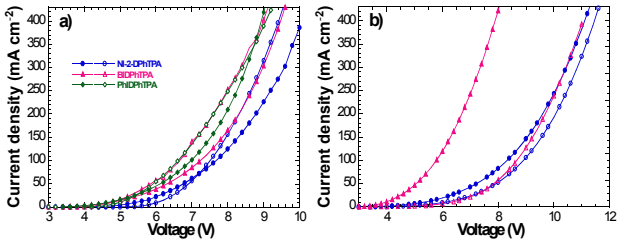

Figure 2. Current density-voltage (J-V) characteristics of the carrier-only devices in configurations of a) ITO/ NPB (40 nm)/ TCTA (5 nm)/ emitter (20 nm)/ NPB (40 nm)/ Al for hole-only devices (*hollow*), and ITO/ TPBi (40 nm)/ emitter (20 nm)/ TPBi (40 nm)/ LiF (1 nm)/ Al for electron-only devices (*solid*), and b) ITO/ HATCN (5 nm)/ emitter (80 nm)/ TAPC (10 nm)/ Al for hole-only devices (*hollow*), and ITO/ TmPyPB (10 nm)/ emitter (80 nm)/ LiF (1 nm)/ Al for electron-only devices (*solid*), where emitter is NI-2-DPhTPA(●○), BIDPhTPA (▲△), or PhIDPhTPA (◆◇).

Multilayer device configuration is commonly adopted for highly efficient OLEDs because it is relatively convenient to tune the carrier transporting and/or to control the exciton distribution by choosing appropriate adjacent materials. Nevertheless, for commercially available OLED applications, it is always highly desirable to simplify the OLED structures and fabrication process greatly further. As has been demonstrated before,[6a] a coordination effect of the exposed nitrogen atom of a compound and LiF would reduce the energy difference between the interface of the compound and the cathode, giving a much better electron injection than these without exposed nitrogen atoms. Then NI-2-DPhTPA and BIDPhTPA with exposed nitrogen atoms were selected to fabricate simplified OLEDs in a configuration of ITO/ HATCN (5 nm)/ emitter (80 nm)/ LiF (1 nm)/ Al, where emitter is NI-2-DPhTPA (marked as S1), or BIDPhTPA (marked as S2). As can be seen in Table 1 and **Figure 3**, both emitters give excellent device performance. In contrast, NI-1-DPhTPA and PhDPhTPA exhibit very poor performance (**Figure S10** and Table S4). Low turn-on voltages and high EQEs have been obtained for devices S1 and S2, exceeding the landmark reports with similar device structures published before.[6a, 9] For the device based on the 1*H*-naphtho[1,2-*d*]imidazole molecule NI-2-DPhTPA, a record-breaking EQE of 4.22% have been achieved with deep blue CIE coordinates of (0.146, 0.104) at 10000 cd m^{-2} and the maximum EQE is 5.12%. The EQE values indicates extremely low EQE roll-off and outstanding performance of the current simplified device. The maximum EQE value of the structure-

Table 1. Summary of the electroluminescent performance of the fabricated non-doped deep blue OLEDs.

Device	V_{on}[a]	CE_{max}	PE_{max}	EQE_{max}	at 1000 cd m^{-2}					at 10000 cd m^{-2}				
	(V)	(cd/A)	(lm/W)	(%)	V (V)	CE (cd/ A)	PE (lm/W)	CIE (x,y)	EQE (%)	V (V)	CE (cd/ A)	PE (lm/W)	CIE (x,y)	EQE (%)
M1	2.6	6.28	7.04	5.92	3.5	6.05	5.44	(0.145, 0.121)	5.70	5.4	5.46	3.21	(0.145,0.117)	5.15
M2	2.6	6.80	7.62	6.18	3.5	6.64	5.96	(0.145, 0.125)	6.03	5.2	5.61	3.39	(0.145,0.121)	5.10
M3	2.6	6.94	7.79	6.43	3.5	6.70	6.01	(0.144, 0.123)	6.21	5.2	5.67	3.43	(0.145,0.120)	5.26
S1	2.6	4.95	4.96	5.12	3.9	4.86	3.96	(0.146, 0.106)	5.02	6.1	4.04	2.08	(0.146,0.104)	4.22
S2	2.6	4.22	4.34	4.40	4.1	3.44	2.64	(0.148, 0.101)	3.39	8.6	1.06	0.69	(0.150,0.087)	1.11

[a]at a luminance of 1 cd m^{-2}.

View Article Online
DOI: 10.1039/C6CC08501F

simplified device apparently reach the EQE limit of traditional fluorescent OLEDs for the first time (5.0 ~ 7.5%, assuming the light out-coupling factor η_{op} = 0.2 ~ 0.3) and the result is comparable with most multilayer non-doped blue devices,[10] demonstrating a bright prospect of the simplified OLEDs. For the BIDPhTPA based device, unfortunately, the EQE value drops sharply compared with the device based on NI-2-DPhTPA and remains only 1.11% at 10000 cd m^{-2}. These data indicate that the injected holes and electrons should be much more imbalanced in the devices based on BIDPhTPA than in the devices based on NI-2-DPhTPA.

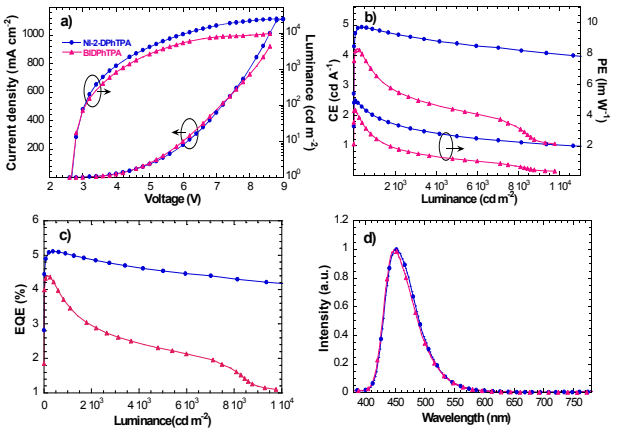

Figure 3. a) Current density and luminance versus driving voltage (J-V-L), b) current efficiency and power efficiency versus luminance (CE-L-PE), c) external quantum efficiency versus luminance (EQE-L) characteristics, and d) electroluminescence (EL) spectra at a 10 mA cm^{-2} of the simplified non-doped OLEDs in a structure of ITO/ HATCN (5 nm)/ emitter (80 nm)/ LiF (1 nm)/ Al, where emitter is NI-2-DPhTPA (●, marked as S1), or BIDPhTPA (▲, marked as S2).

Single-carrier devices with single layer structure were also fabricated and characterized (**Figure 2b**). It turns out that both holes and electrons could be easily injected into the emitters, and the hole currents perform very similar while the situations for the electron injection from the LiF/Al cathode and transport in each material appeared to be quite different, even though their LUMO levels are pretty alike. The big difference should be ascribed to the coordination effect between the exposed nitrogen atom of BIDPhTPA and LiF, which should be stronger than that of NI-2-DPhTPA for its smaller spacial hindrance (Scheme 1, Figure S1, and Figure S6), reducing the energy difference between the interface of BIDPhTPA and the cathode, resulting in better electron injection, leading to unbalanced carriers and thus rapid efficiency roll-off. In addition to the excellent efficiency performance, bluer emission can also be seen from the CIE coordinates (Table 1) and EL spectra (**Figure S11**). This may be ascribed to the microcavity effect, which generally lead to narrower EL spectra.[11]

In summary, a series of deep blue emitters were designed and synthesized for the fabrication of non-doped OLEDs. All the multilayer devices exhibited excellent performances with remarkable EQEs exceeding 5.10% at 10000 cd m^{-2} and extremely reduced efficiency roll-off, which is the best result reported by far. For the simplified single layer devices excluding any charge carrier transporting materials, an unprecedented EQE of 4.22% was achieved at 10000 cd m^{-2} for NI-2-DPhTPA, which can even rival the reported multilayer non-doped deep blue OLEDs. Without utilizing any charge carrier transporting materials, this fabricated deep-blue fluorescent OLEDs with brand new record performance and extraordinary simple device structure can be very promising for future cheap and large scale OLED application at high luminance.

The authors greatly appreciate the financial support from the National Key Research and Development Plan (2016YFB0401004), 973 Project (2015CB655003), the National Natural Science Foundation of China (51625301, 51573059 and 91233116), and Guangdong Provincial Department of Science and Technology (2016B090906003).

Notes and references

1 (a) M. A. Baldo, D. F. O'Brien, Y. You, A. Shoustikov, S. Sibley, M. E. Thompson, S. R. Forrest, *Nature,* 1998, **395**, 151; (b) S.-J. Su, E. Gonmori, H. Sasabe, J. Kido, *Adv. Mater.,* 2008, **20**, 4189.

2 (a) H. Uoyama, K. Goushi, K. Shizu, H. Nomura, C. Adachi, *Nature,* 2012, **492**, 234; (b) G. Z. Xie, X.-L. Li, D. J. Chen, Z. H. Wang, X. Y. Cai, D. C. Dr. Chen, Y. C. Li, K. K. Liu, Y. Cao, S.-J. Su, *Adv. Mater.,* 2016, **28**, 181.

3 (a) Y. Sun, N. C. Giebink, H. Kanno, B. Ma, M. E. Thompson, S. R. Forrest, *Nature,* 2006, **440**, 908; (b) Q. Zhang, J. Li, K. Shizu, S. Huang, S. Hirata, H. Miyazaki, C. Adachi, *J. Am. Chem. Soc.,* 2012, **134**, 14706.

4 (a) J. Lee, H.-F. Chen, T. Batagoda, C. C., D. P. I., M. E. Thompson, S. R. Forrest, *Nat. Mater.,* 2016, **15**, 92; (b) T. Hatakeyama, K. Shiren, K. Nakajima, S. Nomura, S. Nakatsuka, K. Kinoshita, J. Ni, Y. Ono, T. Ikuta, *Adv. Mater.,* 2016, **28**, 2777; (c) X.-L. Li, G. Xie, M. Liu, D. Chen, X. Cai, J. Peng, Y. Cao, S.-J. Su, *Adv. Mater.*, 2016, **28**, 4614.

5 Y.-H. Chen, C.-C. Lin, M.-J. Huang, K. Hung, Y.-C. Wu, W.-C. Lin, R.-W. Chen-Cheng, H.-W. Lin, C.-H. Cheng, *Chem. Sci.,* 2016, **7**, 4044.

6 (a) M. Liu, X.-L. Li, D. C. Chen, Z. Xie, X. Cai, G. Xie, K. Liu, J. Tang, S.-J. Su, Y. Cao, *Adv. Funct. Mater.,* 2015, **25**, 5190; (b) X. Ouyang, X.-L. Li, L. Ai, D. Mi, Z. Ge, S.-J. Su, *ACS Appl. Mater. Inter.,* 2015, **7**, 7869.

7 (a) W.-C. Chen, Y. Yuan, G.-F. Wu, H.-X. Wei, L. Tang, Q.-X. Tong, F.-L. Wong, C.-S. Lee, *Adv. Opt. Mater.,* 2014, **2**, 626; (b) S. Zhang, L. Yao, Q. Peng, W. Li, Y. Pan, R. Xiao, Y. Gao, C. Gu, Z. Wang, P. Lu, F. Li, S. J. Su, B. Yang, Y. Ma, *Adv. Funct. Mater.,* 2015, **25**, 1755; (c) C. Liu, Q. Fu, Y. Zou, C. Yang, D. Ma, J. Qin, *Chem. Mater.*, 2014, **26**, 3074; (d) Y. Zou, J. Zou, T. Ye, H. Li, C. Yang, H. Wu, D. Ma, J. Qin, Y. Cao, *Adv. Funct. Mater.*, 2013, **23**, 1781; (e) M. Zhu, C. Yang, *Chem. Soc. Rev.*, 2013, **42**, 4963.

8 P.-Y. Chou, H.-H. Chou, Y.-H. Chen, T.-H. Su, C.-Y. Liao, H.-W. Lin, W.-C. Lin, H.-Y. Yen, I.-C. Chen, C.-H. Cheng, *Chem. Commun.,* 2014, **50**, 6869.

9 X.-L. Li, X. Ouyang, D. Chen, X. Cai, M. Liu, Z. Ge, Y. Cao, S. J. Su, *Nanotechnology,* 2016, **27**, 124001.

10 (a) W. Li, D. Liu, F. Shen, D. Ma, Z. Wang, T. Feng, Y. Xu, B. Yang, Y. Ma, *Adv. Funct. Mater.,* 2012, **22**, 2797; (b) Y. Li, Z. Wang, X. Li, G. Xie, D. Chen, Y.-F. Wang, C.-C. Lo, A. Lien, J. Peng, Y. Cao, S.-J. Su, *Chem. Mater.,* 2015, **27**, 1100; (c) J. Ye, C. J. Zheng, X. M. Ou, X. H. Zhang, M. K. Fung, C. S. Lee, *Adv. Mater.,* 2012, **24**, 3410.

11 A. Dodabalapur, L. J. Rothberg, R. H. Jordan, T. M. Miller, R. E. Slusher, J. M. Phillips, *J. Appl. Phys.,* 1996, **80**, 6954.